

Thermodynamics of $f(R)$ Theories of Gravity

C.D. Peralta^{1,*} and S.E. Jorás^{2,†}

¹*Instituto de Física, Universidad de Antioquia, Medellín, Colombia*

²*Instituto de Física, Universidade Federal do Rio de Janeiro,
CEP 21941-972 Rio de Janeiro, RJ, Brazil*

This paper starts from a toy model for inflation in a class of modified theories of gravity in the metric formalism. Instead of the standard procedure — assuming a non-linear Lagrangian $f(R)$ in the Jordan frame — we start from a simple ϕ^2 potential in the Einstein frame and investigate the corresponding $f(R)$ in the former picture. The addition of an ad-hoc Cosmological Constant in the Einstein frame leads to a Thermodynamical interpretation of this physical system, which allows further insight on its (meta)stability and evolution.

I. INTRODUCTION

Modified theories of gravity are ordinarily used to replace either the cosmological constant or the inflaton field — explaining, respectively, the current and the early accelerated phase of expansion of the universe. Nevertheless, they were introduced[1] long before any experimental data on either subject were available, just for the sake of completeness and diversity.

In this paper we focus on $f(R)$ theories [2–4] — non-linear functions of the Ricci scalar R defined, as usual, in the Jordan Frame (JF). We follow the metric formalism, which features an extra degree of freedom (d.o.f), as we will briefly review. It is well known that, upon a suitable conformal transformation (as we will also recall below), the modified gravitational Lagrangian assumes the usual Einstein-Hilbert form and the extra d.o.f. is materialized as a scalar field — for obvious reasons, this is the so-called Einstein Frame (EF).

Here, we will follow the same path, but in the opposite direction: we start from a standard ϕ^2 potential with an *ad-hoc* Cosmological Constant Λ in the EF (with also standard slow-roll initial conditions) and investigate the corresponding $f(R)$ in the JF. The introduction of Λ will lead us to a full thermodynamical approach to $f(R)$ theories, shedding some light on the evolution of the system in both frames.

We will now briefly review the aforementioned conformal transformation and the mapping from the quantities defined in one frame to their corresponding *Dopelgänger*s in the other frame.

II. CONFORMAL TRANSFORMATION AND THE INVERSE PROBLEM

From now on, the super(sub)scripts “ E ” and “ J ” indicate the frame (Einstein and Jordan, respectively) where the quantity is defined. We drop the subscript in R_J (and

in ϕ_E — see below) to avoid excessive cluttering of the equations. We write the modified gravitation Lagrangian in JF (in the vacuum, i.e, no matter/radiation fields) as

$$L_J = \sqrt{-g^J} f(R), \quad (1)$$

where $g^J \equiv \det(g_{\mu\nu}^J)$. General Relativity (GR) with a cosmological constant Λ would correspond to $f(R) = R - 2\Lambda$. The standard variational procedure in the metric formalism yields fourth-order equations for the metric [5]

$$R_{\mu\nu} f' - \frac{1}{2} g_{\mu\nu}^J f + g_{\mu\nu}^J \square f' - \nabla_\mu \nabla_\nu f' = 0, \quad (2)$$

where $f' \equiv df/dR$.

One then introduces the new pair of variables $\{g_{\mu\nu}^E, p\}$, related to $g_{\mu\nu}^J$ (and to its derivatives) by a conformal transformation from the JF to the EF[6, 7]:

$$g_{\mu\nu}^E \equiv \Omega^2(x^\alpha) g_{\mu\nu}^J, \quad \text{where} \quad \Omega^2 \equiv p \equiv f'(R). \quad (3)$$

We now define $R(p)$ as a solution of the equation $f'[R(p)] - p = 0$. This procedure corresponds to a standard Legendre Transformation. As such, the expression $R(p)$ is uniquely defined as long as $f'' \equiv d^2 f/dR^2$ has a definite sign. Nevertheless, it is possible to write a unique expression for $R(\phi)$ — see Eq. (7) below — which holds across the branches where $f''(R)$ has different signs, and yields smooth functions $R(t)$ and $\phi(t)$ across the three branches.

A scalar field $\phi_E \equiv \phi$ (dropping the subscript) is traditionally defined in the EF by $p \equiv \exp(\beta\phi)$, with $\beta \equiv \sqrt{2/3}$. The Lagrangian (1) can then be recast in a more familiar form:

$$L_E = \sqrt{-g^E} \left[R_E - g_E^{\mu\nu} \phi_{,\mu} \phi_{,\nu} - 2V_E(\phi) \right], \quad (4)$$

where R_E is the Ricci scalar obtained from $g_{\mu\nu}^E$. In other words, in the EF, the gravitational dynamics is set by a GR-like term (R_E) and the field ϕ is an ordinary minimally-coupled massive scalar field subject to the potential [6]

$$V_E(\phi) \equiv \frac{1}{2p^2} \left\{ p(\phi) R[p(\phi)] - f[R(p(\phi))] \right\} \quad (5)$$

* cesar.peralta@udea.edu.co

† joras@if.ufrj.br

which is completely determined by the particular $f(R)$ chosen.

In the present work we start by examining the inverse problem: from a scalar field ϕ and its potential $V_E(\phi)$, we map L_E in Eq. (4) onto the corresponding L_J in Eq. (1). Following an established procedure [6], one arrives at the following parametric expressions:

$$f(\phi) = e^{2\beta\phi} \left[2V_E(\phi) + 2\beta^{-1} \frac{dV_E(\phi)}{d\phi} \right] \quad \text{and} \quad (6)$$

$$R(\phi) = e^{\beta\phi} \left[4V_E(\phi) + 2\beta^{-1} \frac{dV_E(\phi)}{d\phi} \right]. \quad (7)$$

We will apply the above equations to the simplest possible (nontrivial) potential for a scalar field, to which we add an *ad hoc* Cosmological Constant Λ , namely

$$V_E(\phi) = \frac{1}{2} m_\phi^2 (\phi - a)^2 + \Lambda. \quad (8)$$

For now, Λ and a are written just for the sake of completeness, but they will turn out to be key ingredients later on. We then obtain the corresponding parametric form of $f(R)$:

$$f(\phi) = e^{2\beta\phi} \left[m_\phi^2 (a - \phi) \left(a - \phi - \frac{2}{\beta} \right) + 2\Lambda \right] \quad (9)$$

$$R(\phi) = 2e^{\beta\phi} \left[m_\phi^2 (a - \phi) \left(a - \phi - \frac{1}{\beta} \right) + 2\Lambda \right], \quad (10)$$

which we plot in Fig. 1. If $\Lambda < \Lambda_c$ (to be defined later on), the curve features a 3-branch structure. Throughout the paper, we will refer to those three stages as *branches* of the system. In all of them, from the above expressions, one has $df/dR \equiv f' = \exp(\beta\phi) > 0$. In particular, on the final branch, when the field ϕ oscillates around its potential minimum ($\phi = a$), one recovers GR only if $f' = \exp(\beta a) = 1$, i.e, if $a = 0$. Regardless of a , the system does reach a de Sitter state with a non vanishing $R = R_{\text{dS}} \equiv 4\Lambda \exp(\beta a)$ and, therefore, a corresponding effective cosmological constant in the JF, given by $\Lambda_J \equiv \Lambda \exp(2\beta a)$, and an effective gravitational constant $G_{\text{eff}} \equiv G_N \exp(-\beta a)$, where G_N is the standard gravitational constant. In other words, at the final stage ($\phi \approx a$), the modified Lagrangian given by Eqs. (9) and (10) can be written as the linear function $f(R) = \exp(\beta a)R - 2\Lambda_J$.

The behaviour of $f(R)$ for different values of Λ is shown in Fig. 2 — two slices with $\Lambda = 0$ and $\Lambda = 1.2$ are shown in Fig. 1 (left panels). The attentive reader may recognize a similar surface for the van der Waals gas [8] (vdW, from now on). Indeed, Fig. 2 bears strong resemblance to the Gibbs potential G for the vdW gas as a function of its temperature T and its pressure P . The self-intersecting line indicates the coexistence curve of two phases and the pair of sideways peaks correspond to the metastable states.

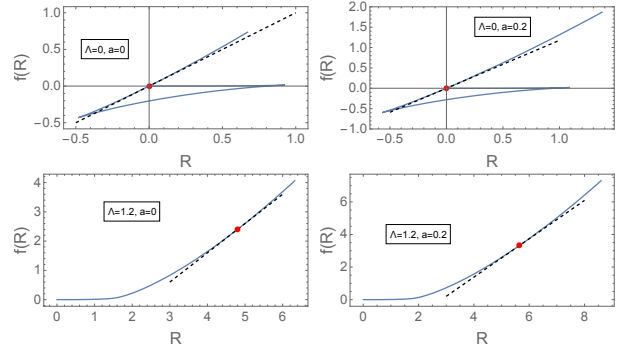


FIG. 1. Parametric plots of $f(R)$ given by Eqs. (9,10) for $\phi \in [-15, 0.5]$ and for the parameters $\{\Lambda, a\}$ shown in the respective insets. In all panels, $f' > 0 \forall R$. The change in a only re-scales the plot. Note that the panels with low Λ present a 3-branch structure. In all of them, the red dot indicates the de Sitter solution (Minkowski, if $\Lambda = 0$) reached when $\phi = a$ and the dashed line is given by $f(R) = \exp(\beta a)R - 2\Lambda_J$, the linear behavior of f at this point.

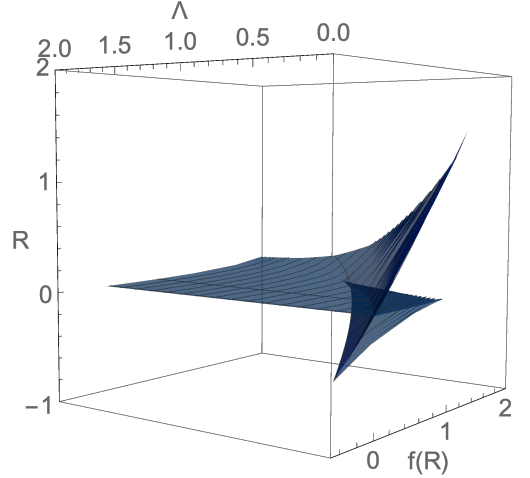


FIG. 2. Plot of $f(R, \Lambda)$, given by Eqs. (9) and (10), with $\beta = \sqrt{2/3}$ and $a = 0$.

III. THERMODYNAMICS

The mere similarity between Fig. 2 and the Gibbs potential might be just a coincidence. Nevertheless, there is indeed a deeper connection: the whole system — its equilibrium points, stability and evolution — is determined by the Gibbs potential and its critical points, as we will now see.

For now, let us associate the Cosmological Constant Λ to an “effective temperature” $T \equiv \Lambda$. On the other hand, we do not directly identify G to f and neither P to R . We rather use an slightly more general *Ansatz*: we define a new pair of coordinates $\{G, P\}$ as a rotation of the original one $\{f, R\}$:

$$\begin{pmatrix} G \\ P \end{pmatrix} \equiv \begin{pmatrix} \cos \theta & -\sin \theta \\ \sin \theta & \cos \theta \end{pmatrix} \begin{pmatrix} f \\ R \end{pmatrix} \quad (11)$$

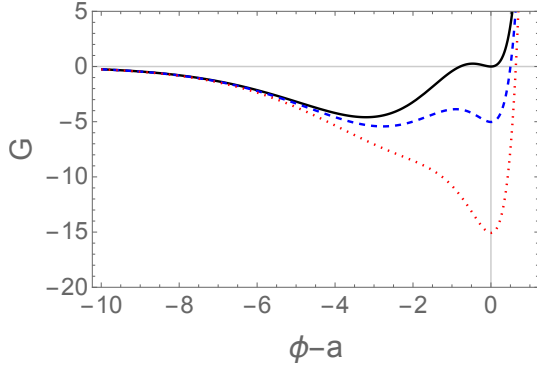


FIG. 3. Plot of Gibbs potential G as a function of $\phi - a$, for $\beta = \sqrt{2/3}$, $\theta = \theta_*$ and $T = 0$ (solid black), $T = 0.5$ (dashed blue) and $T = 1.5$ (dotted red). The minimum at $\phi = a$ always corresponds to $V = 0$ (See Eq. (16) below).

In order to define the exact correspondence, i.e., the

value of θ , we only require that the Gibbs potential, when written as a function of ϕ , always yields a minimum at $\phi = a$, since the field ϕ does oscillate around $\phi = a$, at the end of its evolution. Indeed, such procedure yields $\theta = \theta_* \equiv -\arccos[-(e^{2\beta a} + 1)^{-1/2}]$ and the plot in Fig. 3 for different values of T . There are (for low temperatures), two minima of the Gibbs potential. As T increases, they exchange the dominance until, at $T = T_c \equiv 5/(8\beta^2) = 15/16$, the local minimum and the local maximum coalesce and annihilate each other. Interestingly enough, for low temperatures, the final position of the field $\phi = a$ is *not* the global minimum.

One might acknowledge the existence of another equilibrium point, although an asymptotic one: a local maximum at $\phi \rightarrow -\infty$, which corresponds to an unstable configuration from where the system evolves towards the global minimum.

We will assume $\theta = \theta_*$ from now on and then write a parametric expression for the Gibbs Potential $G(P, T)$:

$$G(\phi, T) = \frac{(\phi - a)e^{\beta\phi} \left\{ e^{\beta\phi} [\beta(\phi - a) + 2] - 2e^{\beta a} [\beta(\phi - a) + 1] \right\} + 2\beta T e^{\beta\phi} (e^{\beta\phi} - 2e^{\beta a})}{\beta \sqrt{e^{2\beta a} + 1}} \quad (12)$$

$$P(\phi, T) = \frac{e^{\beta\phi}}{\beta \sqrt{e^{2\beta a} + 1}} \left\{ e^{\beta(a+\phi)} \left[a^2 \beta - 2a(\beta\phi + 1) + \beta(2T + \phi^2) + 2\phi \right] + \right. \quad (13)$$

$$\left. + 2 \left[a^2 \beta - a(2\beta\phi + 1) + \beta(2T + \phi^2) + \phi \right] \right\}. \quad (14)$$

The effective volume V is the variable “canonically conjugated” to the effective pressure P , i.e., since

$$dG(P, T) = V \cdot dP - S \cdot dT, \quad (15)$$

one can define an effective “volume”

$$V \equiv \left. \frac{\partial G}{\partial P} \right|_T = \left. \frac{\partial G / \partial \phi}{\partial P / \partial \phi} \right|_T = \frac{e^{\beta\phi} - e^{\beta a}}{e^{\beta(a+\phi)} + 1}, \quad (16)$$

from which one can find its minimum value (when $\phi \rightarrow -\infty$): $V_{\min} \equiv -\exp(\beta a)$. Consequently, this so-called “volume” is *not* positive definite. As it is not an actual volume, we see no problem in this feature.

Equations (14) and (16) yield the equation of state for our vdW-like “effective gas”, i.e., an expression that relates P , V and T :

$$P = \frac{(e^{\beta a} + V)}{\beta^2 \sqrt{e^{2\beta a} + 1} (V e^{\beta a} - 1)^2} \left\{ \beta \left[2a^2 \beta + e^{2\beta a} (a^2 \beta - 2a + 2\beta T) - \beta V e^{\beta a} (a^2 + 2T) - 2a + 4\beta T \right] + \right. \quad (17)$$

$$\left. + \log \left(\frac{e^{\beta a} + V}{1 - V e^{\beta a}} \right) \left[-4\beta a - 2e^{2\beta a} (\beta a - 1) + 2\beta a V e^{\beta a} + (e^{2\beta a} - e^{\beta a} V + 2) \log \left(\frac{e^{\beta a} + V}{1 - V e^{\beta a}} \right) + 2 \right] \right\}.$$

The behaviour of $P(V)$ for four different values of T is

shown in Fig. 4, which bears strong resemblance to a

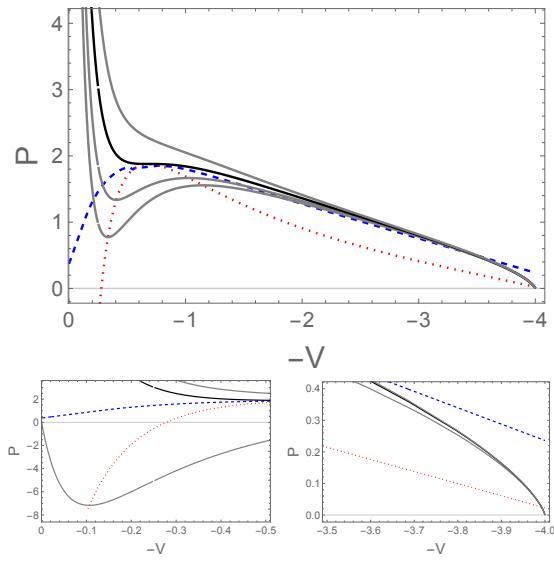


FIG. 4. **All panels:** Plot of the effective pressure P as a function of the (negative) effective volume $-V$, for $a = a_* \equiv 1/\beta$ and different values of temperature: $T = T_c \equiv 15/16$ (solid thick black); lower (higher) curves, in solid thin gray, correspond to lower (higher) temperatures. The spinodal curve is plotted in dotted red. The binodal curve is plotted in dashed blue. **Lower panels:** zooming into opposite ends of the volume axis to show the behavior of the $T = 0$ curve (lowest gray one, not shown in the main panel).

vdW gas. [9] Accordingly, we can define the binodal and spinodal curves, that indicate, respectively, the regions of metastability and instability of the system — see Fig. 4. The former was obtained using two equivalent calculations — from the self-intersecting points of the Gibbs function and from the Maxwell construction — confirming the results from each other. The latter curve is obtained from the extrema of the Gibbs function (see Fig. 1), i.e, the first two turning points (extrema) of $R(t)$. The *critical point* $\{P_c, T_c, V_c\}$, defined at the crossing of those curves, indicates the end of the coexistence line. We will come back to those curves in the next section.

Equation (15) would allow a prompt determination of an analytical expression for the effective Entropy (from $S = -\partial G/\partial T|_P$) if we had an explicit expression $G(P, T)$ (we recall that a constant ϕ does not imply a constant P). Since we do not, we first calculate the Helmholtz Energy $F(V, T) \equiv G(P, T) - P \cdot V$, from which we obtain the entropy $S(V, T)$:

$$S(V, T) \equiv - \left. \frac{\partial F}{\partial T} \right|_V = - \frac{2(e^{a\beta} + V)^2}{\sqrt{e^{2a\beta} + 1}(Ve^{a\beta} - 1)}. \quad (18)$$

One can then realize that the specific heat at constant volume vanishes, since $C_V \equiv T \cdot \partial S/\partial T|_V = 0 \forall T$.

The entropy as a function of pressure and temperature provides another very important piece of information. $S(P, T)$ is depicted in Fig. 5, which also shows the spinodal and binodal curves. The region where the

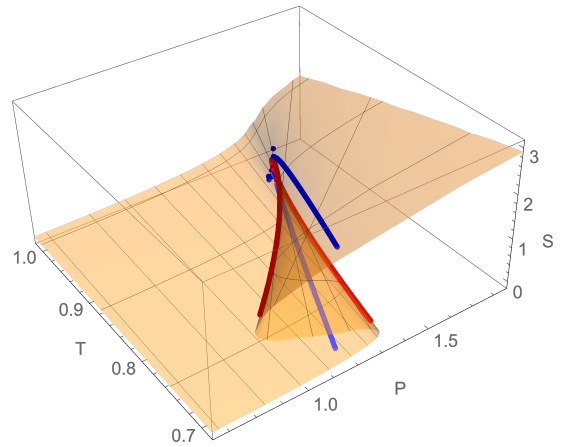


FIG. 5. Surface given by $S(P, T)$ for $a = a_*$. The spinodal and binodal curves are indicated in red (horizontal “Λ” shape) and blue (vertical “U” shape), respectively.

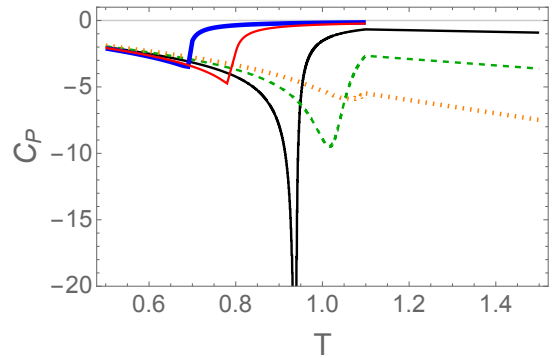


FIG. 6. Behavior of the specific heat at constant pressure C_P as a function of the temperature T close to its transition value ($T_c = 15/16 \approx 0.94$ if $P = P_c$), for different values of pressure (from left to right): $0.85P_c$ (thick blue), $0.9P_c$ (red), P_c (solid black), $1.2P_c$ (dashed green) and $1.2P_c$ (dot-dashed orange). In all curves, $a = a_*$, for which $P_c \approx 1.51$.

entropy is multi-valued is known in Catastrophe Theory [10] as a cusp and indicates the existence of a first-order phase transition and unstable configurations. From $S(P, T)$ we can get the specific heat at constant pressure, $C_P \equiv T \cdot \partial S/\partial T|_P$, shown in Fig. 6. Negative values are expected even in standard gravity theories [11]. We obtain the expected behavior for temperatures around the coexistence curve, for pressures both below (finite jump) and above (smooth behavior) the critical value. We also obtain the usual divergence at the critical point $\{T_c, P_c\}$ (solid black line in Fig. 6) as given by $C_P|_{P_c} \sim [(T_c - T)/T_c]^\alpha$, with $\alpha \approx -1.02$.

IV. A NUMERICAL EXAMPLE

From now on, we will investigate the potential given in Eq. (8) as a standard toy-model inflationary potential

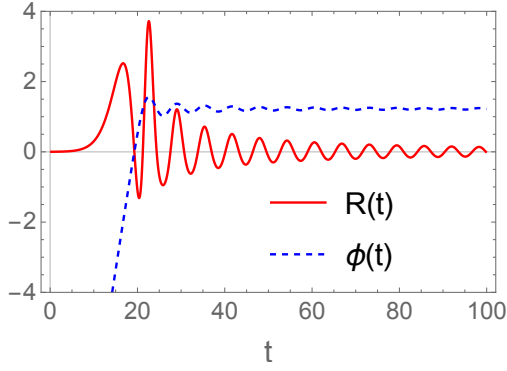


FIG. 7. Numerical solution for $R(t)$ (red/solid) and $\phi(t)$ (blue/dashed), given by Eq. (10) and the numerical solution of Eq. (19), respectively, with $N = 60$ e-folds, using the potential defined in Eq. (8), with $m_\phi = 1$, $\Lambda = 0$ and $a = a_*$.

in the EF — initially, we will keep $a = \Lambda = 0$. We would like to determine the time evolution of $R(t)$ and $\phi(t)$. We recall that throughout this paper there is no matter nor radiation; the ϕ field is pure gravity. In GR, that would imply $R = 0 \forall t$. In $f(R)$ theories, on the other hand, R has a dynamical behavior of its own. Here, it suffices to use $R[\phi(t)]$ (defined in the JF) from Eq. (10) and $\phi(t)$ (in the EF) from the standard equation of motion for a scalar field in an expanding homogeneous spacetime:

$$\ddot{\phi}(t) + 3H(t)\dot{\phi}(t) + V'_E[\phi(t)] = 0, \quad (19)$$

where $V'_E \equiv dV_E/d\phi$ and $H^2(t) = \{\dot{\phi}(t)^2/2 + V_E[\phi(t)]\}/3$. The initial conditions for the numerical solution of Eq. (19) are the standard ones in the slow-roll approximation [12]: $\phi(0) = -\sqrt{2(1+2N)} \approx -15.5$ and $\dot{\phi}(0) = \sqrt{2/3} \approx 0.81$, which correspond to $R(0) \approx 3.4 \times 10^{-3}$ and $\dot{R}(0) \approx 1.8 \times 10^{-3}$ [13].

One can follow the evolution of the system along Fig. 1 (top panels): The system starts close to the origin and slowly moves along the first branch (close to the horizontal axis), generating an initially inflationary phase (since $R \approx \text{const}$). It then quickly sweeps through the second branch (where $f'' < 0$) and then oscillates around the origin along the almost-linear third branch (where GR is recovered for $a = 0$).

Accordingly, in Fig. 3, the system starts close to the unstable equilibrium point (therefore, a naturally momentary inflationary phase), visits the global minimum (the first turnaround point of $R(t)$, where $R'(t) = 0$) and finally settles down at the local minimum $\phi = a$. Only for larger values of $T \equiv \Lambda$, the final solution (always at $\phi = a \Leftrightarrow R = 8\Lambda \exp(\beta a)$) is the *global* minimum.

The same behavior can be seen in Fig. 4: the system always starts at $V \approx -4$, in the unstable region (in the lower right panel, one can see all the curves, regardless of T , inside the spinodal region). The effective fluid momentarily visits the (meta)stable gas phase (large V , low P) and then oscillates around the local minimum (for low T) that corresponds to the liquid phase (low V , large P).

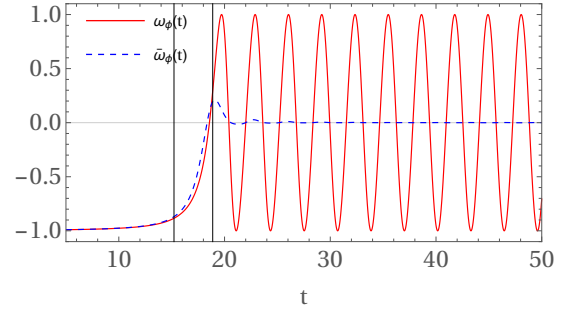


FIG. 8. Equation-of-state parameter (w_ϕ and its time average \bar{w}_ϕ) for the ϕ field, defined in the EF, as functions of time, for $\Lambda = 0$. The vertical lines correspond to $t = t_1$ and $t = t_2$, when $\dot{R}(t_1) = \dot{R}(t_2) = 0$, i.e., at the sideways peaks in Fig. 1 (top panels).

Then at the final configuration, when $V = 0$ (see lower left panel), the system (still for low T) is between the binodal and spinodal curves, signaling a metastable configuration — which matches the *local* minimum at $\phi = a$ in Fig. 3 for $T = 0$. For higher temperatures, though, the curve is above the binodal line at $V = 0$, which happens when the final configuration is a *global* minimum.

Each description above explains the same evolution from a different point of view; each one uses a different — but equivalent — fluid, as we shall see now.

A. Einstein Frame (EF)

We plot in Fig. 8, along each of such aforementioned periods, the corresponding equation-of-state parameter for the ϕ field (defined in the EF):

$$w_\phi(t) \equiv \frac{p_\phi(t)}{\rho_\phi(t)} \equiv \frac{\frac{1}{2}\dot{\phi}^2 - V_E[\phi(t)]}{\frac{1}{2}\dot{\phi}^2 + V_E[\phi(t)]}, \quad (20)$$

and its average over one period T (defined in the final oscillatory phase). There are clearly two distinct phases: the early inflationary period, characterized by $w_\phi \approx \bar{w}_\phi \approx -1$, and the dust-like phase, when w_ϕ oscillates between ± 1 and $\bar{w}_\phi = 0$, as for the traditional inflaton field in the JF [14]. The sideways peaks, at $t_{1,2}$, indicate the transition between the aforementioned phases.

B. Jordan Frame (JF)

There is a corresponding behavior in the JF, of course. One can define a “curvature fluid” whose energy density and pressure are, respectively:

$$8\pi G\rho_c \equiv (f'R - f)/2 - 3H\dot{f}' + 3H^2(1 - f') \quad (21)$$

$$8\pi Gp_c \equiv \ddot{f}' + 2H\dot{f}' - (2\dot{H} + 3H^2)(1 - f') + (f - f'R)/2. \quad (22)$$

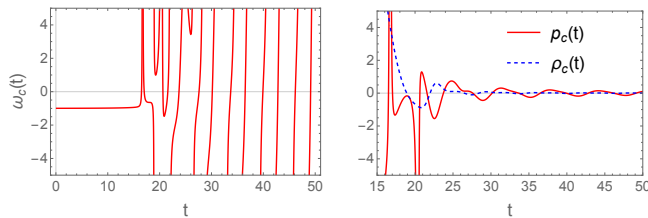


FIG. 9. **Left panel:** Equation-of-state parameter ω_c for the “curvature fluid” in the JF as a function of time. The divergences, all of them non-physical, correspond to $\rho_c = 0$, which happens periodically while the field ϕ oscillates around the minimum of its potential $V_E(\phi)$. **Right panel:** Corresponding pressure p_c (red solid curve) and density ρ_c (blue dashed line) for the “curvature fluid”, as a function of time. In **both panels**, $\Lambda = 0$ and $a = a_*$.

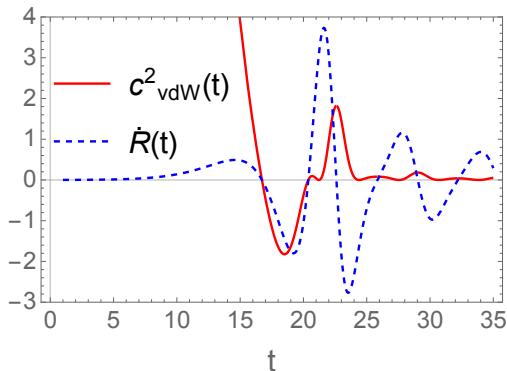


FIG. 10. Plot of $\dot{R}(t)$ (dashed blue line) and $c_{\text{vdW}}^2 \equiv \dot{P}/\dot{\rho}$ (solid red curve) for the effective vdW gas, for $T = 0.5$ and $a = a_*$, as functions of time. Notice that $c_{\text{vdW}}^2 < 0$ only between the two sideways peaks in Fig. 1, exactly when $f'' < 0$, as expected. The same behavior is found for all $T < T_c$.

In Fig. 9 we plot the corresponding equation-of-state parameter $\omega_c \equiv p_c/\rho_c$ (left panel), $\rho_c(t)$, $p_c(t)$ (right panel), all of them defined in the JF, for $\Lambda = 0$ and $a = a_*$. In the inflationary phase, the curvature fluid behaves as a cosmological constant ($\omega_c \approx -1$), as expected, since it is responsible for the accelerated quasi-de Sitter expansion. In the oscillatory phase, on the other hand, the behaviour of ω_c is not usual just because ρ_c vanishes periodically, whenever $\phi(t) = 0$ at the bottom of its potential $V_E(\phi)$ — see Fig. 9, right-hand panel. Nevertheless, there are no divergences of *physical* quantities. If $\Lambda \neq 0$, then $\omega_c = \omega_\phi = -1$ also in the final stages, as expected.

C. vdW fluid

Two important pieces of information are available only from the vdW gas and *not* from either the curvature fluid or the ϕ field.

One of them is its sound speed squared, defined as

$c_{\text{vdW}}^2 \equiv \dot{P}/\dot{\rho} = (V^2/|\kappa|)\dot{P}/\dot{V}$ (since $V < 0$, we write $\rho = \kappa/V$, with a constant $\kappa < 0$ so that $\rho > 0$) and plotted in Fig. 10 together with $\dot{R}(t)$. We can see that $c_{\text{vdW}}^2 < 0$ *only* between the first two extrema of $R(t)$, i.e., in the second branch (see Fig. 1), when $f'' < 0$, as expected from the usual *perturbative* argument on stability of $f(R)$ theories [5]. In this phase, fluctuations grow exponentially fast — further details will be the subject of future work. Obviously, for $T > T_c$, the second branch is suppressed and one obtains $c_{\text{vdW}}^2 > 0 \forall t$.

Another important feature is the sudden jump in the entropy — from $S(V_{\min}) = 0$ to $S(V = 0) = 2e^{2\beta a}/\sqrt{e^{2\beta a} + 1} \sim 2e^{\beta a}$ (for large $a > 0$) — marking the release of latent heat, just as expected in an ordinary first-order phase transition, which has already been pointed out by the C_P behavior, shown in the previous section.

V. CONCLUSIONS

We are currently investigating other physical consequences of the approach here presented, that may indicate that either the potential we assume is a simple toy model or that there might be some compatibility with observable quantities from inflation. For instance, during the spinodal decomposition process, only a given range of wavelength is exponentially amplified [15], which is similar to a feature that has already been proposed in the preheating scenario [16].

We also recall that a non vanishing $a > 0$ reduces the value of the effective Newton’s constant and, at the same time, generates a large effective cosmological constant in the JF (see discussion in Section II). In a more speculative note, we hypothesize that such a mechanism could be used to (almost) cancel out a bare Λ_0 in the JF, if $\Lambda < 0$.

In any case, the inverse mapping from EF to JF and the phase transition still stand and may be a key feature in a more detailed model. Indeed, we are currently examining other potentials $V_E(\phi)$ and further generalizations. For instance, the cosmological “constant” in the EF is *not* a dynamical quantity in the present work, but it may become so if it is actually the vacuum energy of another field which happens to go through a phase transition of its own.

SEJ thanks Valerio Faraoni and Thomas Sotiriou, for some clarifying talks in the initial phase of this work, and Robert Brandenberger for important suggestions. CDP thanks Omar Roldan for his kind hospitality, and Diego Restrepo for his support while away from U. Antioquia and acknowledges financial support from COLFUTURO/COLCIENCIAS, Colombia, under the program Becas Doctorados Nacionales 647 and Instituto de Física from U. Antioquia.

-
- [1] G. V. Bicknell, J. Phys. A: Math., Nucl. Gen. **Vol. 7**, **No. 9** (1974).
- [2] A. De Felice and S. Tsujikawa, Living Rev. Rel. **13**, 3 (2010), arXiv:1002.4928 [gr-qc].
- [3] S. Capozziello and M. De Laurentis, Phys. Rept. **509**, 167 (2011), arXiv:1108.6266 [gr-qc].
- [4] S. Nojiri, S. D. Odintsov, and V. K. Oikonomou, Phys. Rept. **692**, 1 (2017), arXiv:1705.11098 [gr-qc].
- [5] T. P. Sotiriou and V. Faraoni, Rev. Mod. Phys. **82**, 451 (2010), arXiv:0805.1726 [gr-qc].
- [6] G. Magnano and L. M. Sokolowski, Phys. Rev. **D50**, 5039 (1994), arXiv:gr-qc/9312008 [gr-qc].
- [7] R. M. Wald, *General Relativity* (Chicago Univ. Pr., Chicago, USA, 1984).
- [8] H. Callen, *Thermodynamics and an Introduction to Thermostatistics* (Wiley & Sons, 2nd Edition, 1985).
- [9] It is tempting to conjecture that the limit $a \rightarrow \infty$ corresponds to the vdW gas (in spite of the negative effective volume) but it can be shown that in the high-temperature limit one gets $P \propto V^{-2}$, instead of the standard $P \propto V^{-1}$.
- [10] P. Saunders, *An Introduction to Catastrophe Theory* (Cambridge University Press, 1980).
- [11] T. Padmanabhan, Physics Reports **188**, 285 (1990).
- [12] A. D. Linde, *22nd IAP Colloquium on Inflation + 25: The First 25 Years of Inflationary Cosmology Paris, France, June 26-30, 2006*, Lect. Notes Phys. **738**, 1 (2008), arXiv:0705.0164 [hep-th].
- [13] Where ϕ is given in Planck-Mass (M_{Pl}) units, R is given in M_{Pl}^4 , and $N = 60$ is the number of e-folds.
- [14] At some point, the inflaton field should couple to matter (which is absent in our model from the beginning) to start (p)reheating — the study of such phase is beyond the scope of the present paper.
- [15] P. Chomaz, M. Colonna, and J. Randrup, Physics Reports **389**, 263 (2004).
- [16] R. Allahverdi, R. Brandenberger, F.-Y. Cyr-Racine, and A. Mazumdar, Annual Review of Nuclear and Particle Science **60**, 27 (2010).